Understanding Recurrent Neural Architectures by Analyzing and Synthesizing Long Distance Dependencies in Benchmark Sequential Datasets

A Preprint

Abhijit Mahalunkar
ADAPT Research Centre
Technological University Dublin
Dublin, Ireland
`abhijit.mahalunkar@tudublin.ie`

John D. Kelleher
ADAPT Research Centre
Technological University Dublin
Dublin, Ireland
`john.d.kelleher@tudublin.ie`

December 9, 2020

Abstract

In order to build efficient deep recurrent neural architectures, it is essential to analyze the complexity of long distance dependencies (LDDs) of the dataset being modeled. In this paper, we present detailed analysis of the dependency decay curve exhibited by various datasets. The datasets sampled from a similar process (e.g. natural language, sequential MNIST, Strictly *k*-Piecewise languages, etc) display variations in the properties of the dependency decay curve. Our analysis reveal the factors resulting in these variations; such as (i) number of unique symbols in a dataset, (ii) size of the dataset, (iii) number of interacting symbols within a given LDD, and (iv) the distance between the interacting symbols. We test these factors by generating synthesized datasets of the Strictly *k*-Piecewise languages. Another advantage of these synthesized datasets is that they enable targeted testing of deep recurrent neural architectures in terms of their ability to model LDDs with different characteristics. We also demonstrate that analysing dependency decay curves can inform the selection of optimal hyper-parameters for SOTA deep recurrent neural architectures. This analysis can directly contribute to the development of more accurate and efficient sequential models.

***K*eywords** Long Distance Dependencies · Sequential Models · Recurrent Neural Networks

1 Introduction

Recurrent Neural Networks (RNN) laid the foundation of sequential data modeling [1]. However, recurrent neural architectures trained using backpropagation through time (BPTT) suffer from exploding or vanishing gradients [2, 3, 4]. This problem presents a specific challenge in modeling sequential datasets which exhibit long distance dependencies (LDDs). LDDs describe an interaction between two (or more) elements in a sequence that are separated by an arbitrary number of positions. LDDs are related to the rate of decay of statistical dependence of two points with increasing time interval or spatial distance between them. This dependence can be computed using information theoretic measure i.e. *Mutual Information* [5, 6, 7, 8]. For example, in English there is a requirement for subjects and verbs to agree, compare: "*The **dog** in that house **is** aggressive*" with "*The **dogs** in that house **are** aggressive*". One of the early attempts at addressing this issue was by [9] who proposed a hierarchical recurrent neural network which introduced several levels of state variables, working at different time scales. Various other architectures were developed based on these principles [10, 11]. Another well-known approach to addressing this challenges is the Long Short-Term Memory (LSTM) introduced by [12]. The LSTM architecture models LDDs by enforcing constant error flow through *constant error carousels* within special units. More recently, attention and memory augmented networks has shown to deliver good performance in modeling LDDs [13, 14, 15], and transformers use self-attention to model LDDs [16, 17].

A fundamental task of modelling sequential data is Language Modeling. A language model accepts a sequence of symbols and predicts the next symbol in the sequence. The accuracy of a language model is dependent on the capacity of the model to capture the LDDs in the data on which it is evaluated because an inability to model LDDs in the input sequence will result in erroneous predictions. In this paper, we reviewed the SOTA language models to check their performance on these datasets. The standard evaluation metric for language models is *perplexity*. Perplexity is the measurement of how well a language model predicts the next symbol, and the lower the perplexity of a model the better the performance of the model. There are a number of benchmark datasets used to train and evaluate language models: Penn TreeBanks (PTB) [18], WikiText2, WikiText103 [13] and Hutter-Text (Text8 and Enwik8).

Our review of the language model SOTA revealed that most research on developing language models fail to explicitly analyze the the LDDs within the datasets used to train and evaluate the models. Motivated by this, the paper makes a number of research contributions. First, we argue that a key step in modeling sequential data is to understand the properties of the LDDs within the data. Second, we present a method to compute and analyze the dependency decay curve for any sequential dataset, and demonstrate this method on a number of datasets that are frequently used to benchmark the SOTA sequential models. Third, based on the analysis of the dependency decay curves, we observe that LDDs are far more complex than previously assumed, and depend on at least four factors: (i) number of unique symbols in a dataset, (ii) size of the dataset, (iii) number of interacting symbols within an LDD, and (iv) distance between the interacting symbols. Fourth, we demonstrate how understanding dependency decay curve can inform better hyper-parameter selection for current SOTA recurrent neural architectures, and also aid in understanding them. We demonstrate this by using Strictly k-Piecewise (SPk) languages as a benchmark task for sequential models. The motivation for using the SPk language modelling task, is that the standard sequential benchmark datasets provide little to no control over the factors which directly contribute to dependency decay curve. By contrast, we can generate benchmark datasets with varying degrees of LDD complexity by modifying the grammar of the SPk language [19, 20, 21].

2 Related Work

Mutual information has previously been used to compute LDDs. Two literary texts, Moby Dick by H. Melville and Grimm's tales were used to analyze maximum length of LDDs present in English text [22]. Correlations were found between few hundred letters. More specifically, strong dependence was observed (large $\alpha 1$) upto 30 characters indicating strong grammar, beyond which point the curve exhibited a long tail indicating weak dependence. Dependency decay curves were analyzed of Enwik8 [8]. It was observed that LDDs with power-law correlations tend to be more difficult to model. They argued that LSTMs are capable of modeling sequential datasets exhibiting LDDs with power law correlations such as natural languages far more effectively than markov models; due to power-law decay of hidden state of the LSTM network controlled by the forget gate. In another experiment, it was observed that DNA nucleotides exhibited long-range power law correlations [23, 24].

Formal Language Theory, primarily developed to study the computational basis of human language is now being used extensively to analyze rule-governed systems [25, 26, 27]. Formal languages have previously been used to train RNNs and investigate their inner workings. The Reber grammar [28] was used to train various 1st order RNNs [29, 30]. The Reber grammar was also used as a benchmark dataset for LSTM models [12]. Regular languages, studied by Tomita [31], were used to train 2nd order RNNs to learn grammatical structures of the strings [32, 33]. Regular languages are the simplest grammars (type-3 grammars) within the Chomsky hierarchy which are driven by regular expressions. Strictly k-Piecewise languages are natural and can express some of the kinds of LDDs found in natural languages [34, 35]. This presents an opportunity of using SPk grammar to generate benchmark datasets [21, 36]. LSTM networks were trained to recognize valid strings generated using SP2, SP4, SP8 grammar [21]. LSTM could recognize valid strings generated using SP2 and SP4 grammar but struggled to recognize strings generated using SP8 grammar, exposing the performance bottleneck of LSTM networks. It was also observed that by increasing the maximum length of the generated strings of SP2 language (increasing the length of LDDs), the performance of LSTM degraded [36].

3 Computing Dependency Decay Curves of Natural Datasets

3.1 Information Theoretic Association Measures

Mutual information is an information-theoretic measure of association that computes the dependence between two or more events or distributions [37, 38, 5]. Pointwise Mutual Information (PMI) computes the dependence between single events x and y belonging to the discrete random variables X and Y respectively by measuring their individual distributions and their joint distributions. PMI is i:

$$i(x; y) = \log \frac{p(x, y)}{p(x)p(y)} \tag{1}$$

Average Mutual Information (MI) computes the dependence between two random variables X and Y with marginal distributions $p(x)$ and $p(y)$ and with the joint distribution $p(x, y)$. MI is the average or expectation over all possible events or PMI. MI is $I(X; Y)$:

$$I(X;Y) = \sum_{x,y} p(x,y) \log \frac{p(x,y)}{p(x)p(y)} \tag{2}$$

MI can also be expressed using the entropy of X and Y, i.e. $H(X)$, $H(Y)$, and their joint entropy, $H(X, Y)$, as:

$$I(X;Y) = H(X) + H(Y) - H(X,Y) \tag{3}$$

$$H(X) = \log N - 1/N \sum_{s=1}^{V} N_s \psi(N_s) \tag{4}$$

Here, N_s is the frequency of unique symbol s, $N{=}\sum N_s$, V is the number of unique symbols or the vocabulary size, and $\psi(N_s)$ is the *digamma function* of N_s. Shannon's entropy is known to be biased, generally underestimating the true entropy from finite samples; that is why, in order to compensate for insufficient sampling we use Eq. 4 from [39] to calculate entropy.

If $I(X; Y){=}0$, then X and Y are independent then $p(x)p(y){=}p(x, y)$. However, if X and Y are fully dependent, then $p(x){=}p(y){=}p(x, y)$, which results in the maximum value of $I(X; Y)$. Similarly, if $i(x; y){=}0$, then events x and y are independent. If $i(x; y)$ is positive, it indicates that the two words occur together frequently. If $i(x; y)$ is negative, it indicates that the two words never occur together.

3.2 Dependency Decay Curve

A dependency decay curve describes how the mutual information between symbols in a dataset decays as the distance between the symbols increases. To compute the dependency decay curve of a dataset we need to compute MI at every distance d in the dataset, where d is the spacing between pair of symbols. This is achieved by designing random variables X and Y, where X holds the subsequence of the original sequence with index range $[0, LEN{-}1{-}D]$, and Y holds the subsequence with index range $[D, LEN{-}1]$ for all $D \in d$; where LEN is the size of the dataset or the original sequence. The figure below illustrates how X and Y are defined over a sequence when $d = 2$.

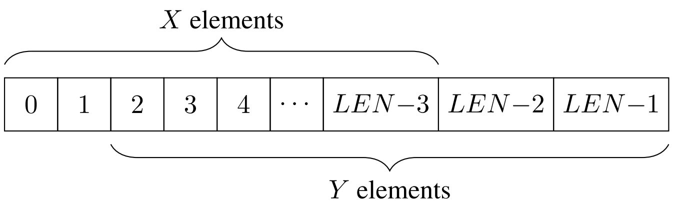

Next we define a random variable XY that contains a sequence of paired symbols one from X and one from Y, where the symbols in a pair have the same index in X and Y. The figure below illustrates the definition of these pairs, each column defines one XY pair.

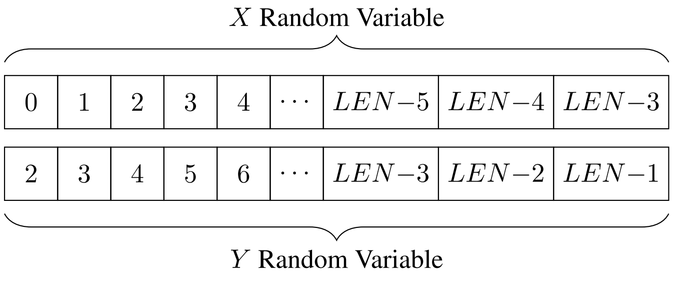

After this, we count the number of symbols that appear in X and Y (i.e., the size of the symbol vocabulary of X and Y) these counts are stored in K^X, K^Y respectively. Similarly, we count the number of unique pairs of symbols in XY and store this in K^{XY}. We then obtain the frequency of each symbol in the vocabularies of X and Y, giving us N_i^X and N_i^Y; and the frequency of each of the pairs of symbols in XY, giving us N_i^{XY}. Using this information, and E.q. 3 and 4, we calculate the mutual information $I(X; Y)$ at a distance D in a sequence. We repeat this process for every $D{\in}d$, where $1{<}d{<}LEN$. The value of $I(X; Y)$ as a function of d is the *Dependency Decay Curve* $I(d)$. The area under the dependency decay curve describes the spread of dependencies along d. This curve is plotted on the log-log axis. The x-axis gives d, and the y-axis gives the MI at that D (measured in *nats*). Algorithm 1 below explains the details.

Algorithm 1 Computing dependency decay curves

```
for $d \leftarrow 1, |dataset|$ do
    $X \leftarrow dataset[0 : |dataset| - D]$
    $Y \leftarrow dataset[D : |dataset|]$
    $XY \leftarrow$ zero-matrix of size $(K^X, K^Y)$
    for $i \leftarrow 0, |X|$ do
        Increment $XY[X[i], Y[i]]$
    end for
    Compute $N_i^X$, $N^X$, $K^X$ for $X$
    Compute $N_i^Y$, $N^Y$, $K^Y$ for $Y$
    Compute $N_i^{XY}$, $N^{XY}$, $K^{XY}$ for $XY$
    Compute $H(X)$, $H(Y)$ and $H(X,Y)$ using Eq. 4
    $I[D] \leftarrow H(X) + H(Y) - H(X,Y)$
end for
Return I[d]
```

3.3 Dependency Decay Curves of Word-Based Datasets

The dependency decay curves of word-based PTB, WikiText2, WikiText103 and Text8 datasets are in Fig. 1 and are plotted on a log-log axis where a straight line represents a power-law. Examining these curves, it is reasonable to describe each of these curves as combining multiple straight-line segments. The figure reveals that in each of these datasets the dependency decay follows multiple power-laws. Multiple power-laws that are combined together can be described using a *broken power-law* relationship, an example of which is presented in Eq. 5. Here the broken power-law function $f(d)$ is comprised of three power-laws with exponents α_1, α_2, and α_3 and corresponding constants c_1, c_2, and c_3, and combined at thresholds d_{b1} and d_{b2}.

$$f(d) = \begin{cases} c_1 * d^{-\alpha_1} & d \leq d_{b1} \\ c_2 * d^{-\alpha_2} & d_{b1} < d \leq d_{b2} \\ c_3 * d^{-\alpha_3} & d > d_{b2} \end{cases} \tag{5}$$

In general, the threshold or *inflection point* that joins any two power-laws is of paramount importance as it indicates a change in a system where one phenomenon gives way to another. For example, in astronomy, the simplest afterglow light curves of the gamma-ray bursts can be described using a broken power-law. Here, the electron energy observed before and after the jet break (threshold) in the observer's frame exhibit different electron energy distribution index (i.e., different power laws) [40, 41]. For natural processes, this transition at the threshold is not sharp and is often replaced with a smoothly joined broken power-law. Eq. 5 is of an ideal broken power-law with sharp discontinuities. To accommodate for smoothing, Eq. 5 needs to be adjusted as below:

$$f_{sm}(d) = \begin{cases} c_1 * d^{-\alpha_1} & d \leq d_{b1} \\ c_2 * d^{-\alpha_2} & d_{r1} < d \leq d_{b2} \\ c_3 * d^{-\alpha_3} & d > d_{r2} \end{cases} \tag{6}$$

Here, the first power-law i.e $c_1{*}d^{-\alpha_1}$ ends at d_{b1} and second power-law i.e. $c_2{*}d^{-\alpha_2}$ begins at d_{r1}. The region between $d_{b1}{<}d{<}d_{r1}$ is a smooth curve joining the two power-laws where the slope of the curve in that region changes from α_1 to α_2. Hence this is the transition region. This also happens between the second power-law and third power-law i.e. $c_3{*}d^{-\alpha_3}$. Here, the second power-law ends at d_{b2} and third power-law begins at d_{r2} and the transition region is between $d_{b2}{<}d{<}d_{r2}$. Bringing the discussion back to the word-based English datasets, if we model the dependency decay exhibited by word-based dataset using equation 6, then d describes the separation or distances between the symbols and c_1 describes the mutual information at a distance of one (d=1) (i.e. it describes the extent of the dependence of a word on its immediate neighbour). Furthermore, α_1 describes the rate of decay of dependence between words as the separation between them d increases, this rate of decay holds until the first inflection point (d_{b1}). Similarly, c_2 describes the mutual information at d_{r1} and α_2 describes the rate of decay of dependence between words as the separation between them increases for $d_{r1}{<}d{\leq}d_{b2}$, and so on. The presence of broken power-law signifies that the dependencies decay at different rates and these changes in decay rates may be caused by interactions between a number of different underlying phenomena.

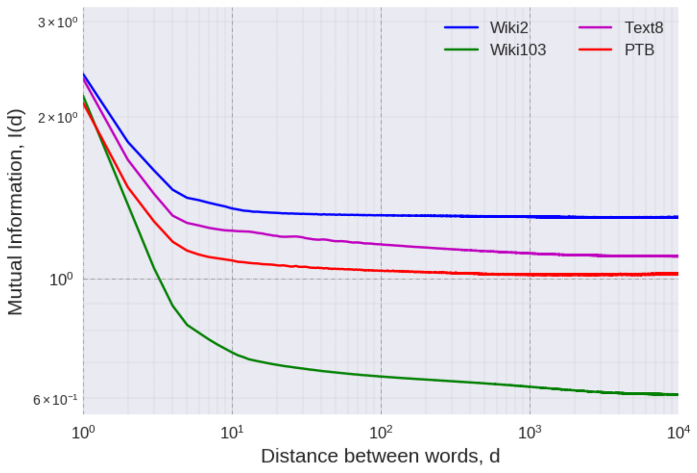

Figure 1: Dependency decay: Word-based dataset

3.3.1 Fitting Word-Based Dependency Decay Curves

To study the properties of LDDs in a given dataset, it is essential to obtain the properties of the dependency decay curves. Fitting to a dependency decay curve involves estimating the values for the thresholds (inflection points) between the component power-laws and the parameters of each component power-law. Unfortunately, we do not have access to a function that can generate a curve with three smooth broken power-laws. Consequently, the process we use involves first fitting a broken power-law combining two power-laws to an initial portion of the observed curve, and then fitting a second broken power-law combining two power-laws to the remainder of the curve. To implement this two-stage curve fitting process we use the *SmoothlyBrokenPowerLaw1D* function (*Astropy* library) to generate a smoothly broken power-law curve from a set of estimated parameters.

$$g(d) = A\left(\frac{d}{d_b}\right)^{-\alpha}\left[\frac{1}{2}+\frac{1}{2}\left(\frac{d}{d_b}\right)^{\frac{1}{\Delta}}\right]^{(\alpha-\alpha^s)\Delta} \tag{7}$$

where, d_b is the threshold (inflection point) connecting the two power-laws, α is the index of the first power-law, α^s is the index of the second power-law, A is the amplitude at the inflection, and Δ is a smoothness parameter which describes the smoothness of the transition between the two power-laws. In this context, the beginning of the transition region is denote by d_l which marks where the transition phenomenon begins, d_b marks the boundary where the relative dominance of the two phenomena switches, and the end of the transition region is denote by d_r, where the transition between the two phenomena is complete. Using these definitions for d_l, d_r, and d_b the relationship between the smoothness parameter Δ and the transition between the two power-laws is:

$$\log_{10}\frac{d_r}{d_b} = \log_{10}\frac{d_b}{d_l} \sim \Delta \tag{8}$$

At values $d \lesssim d_l$ and $d \gtrsim d_r$ the model is approximately a simple power law with index α and α^s respectively. The two power laws are smoothly joined at values $d_l < d < d_r$, hence the Δ parameter sets the "smoothness" of the slope change. However, our experiments reveal that $d_l \approx d_b$, so for all practical purposes, d_l can be replaced by d_b. Eq. 7 does not take c as a parameter and is calculated by the function *SmoothlyBrokenPowerLaw1D*.

In fitting the first broken power-law to a dependency decay curve we selected $I(d)$ where $1<d<700$. This selection was done by examining Fig. 1 and selecting the region of the curve that we were confident included one inflection point and two power-laws. We then generated estimates for the values of α_1, α_1^s, d_{b1}, A_1, and Δ_1, and these estimates were passed as parameters to the Eq. 7 to generate a smoothly broken power-law curve and obtain c_1, d_{l1}, and d_{r1} values. To fit the second broken power-law we used the same process as we used to fit the first broken power-law with the distinction that we fitted the second broken power-law to the region of the dependency decay curve $I(d)$ where $d_{r1}<d<10000$. Here we obtain the value of the parameters of c_2, α_2, α_2^s, A_2, Δ_2, d_{l2}, d_{r2}, and d_{b2}. Finally, the generated curve and the selected portion of the relevant dependency decay curve $I(d)$ were checked for the goodness of fit using the *2-Sample Kolomogrov-Smirnov Test* (*p-value*<0.05). The fitting process is displayed in Fig. 2. The power-law parameters and inflection points are listed in table 1. Note that we do not retain the values for d_{l2} and d_{r2} from the second broken power-law because we found that for all the datasets the inflection point between the two power-laws in the region was very sharp i.e., $d_{b2} \approx d_{l2} \approx d_{r2}$.

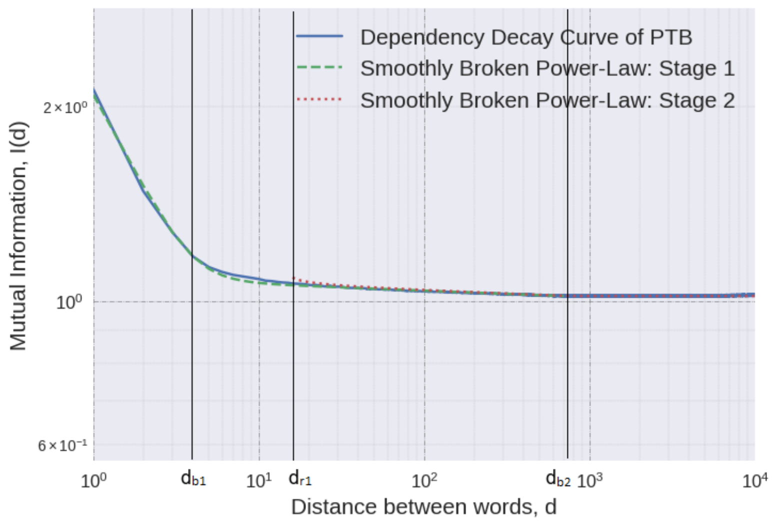

Figure 2: Broken power-law fit: PTB dataset

Datasets	Vocabulary	Size	c_1	α_1	d_{b1}	Δ_1	d_{r1}	c_2	α_2	d_{b2}
PTB	10000	1085779	2.12	0.4786	4	0.275	15	1.1716	0.01	728
Text8	253854	17005208	2.35	0.4811	4	0.228	12	1.309	0.016	951
Wiki2	33278	2551843	2.38	0.421	4	0.346	23	1.463	0.0028	2203
Wiki103	267735	103690236	2.19	0.6931	5	0.35	20	0.821	0.019	2660

Table 1: Broken power-law fitting parameters for word-based datasets

To illustrate how closely the two fitted broken power-laws match the dependency decay curves, Fig. 2 illustrates the fit between the dependency decay curve of PTB and the two smoothly broken-power law curves generated using the above process. In this figure the positions of d_{b1}, d_{r1} (end of the transition region between the first and second power-law), and d_{b2} are shown. Notice that there is a small discontinuity at d_{r1} which marks the joint between the two phases of curve-fitting. However, apart from this discontinuity it is apparent that the fitted curves closely match the curves.

3.3.2 Analysis of Word-Based Datasets

Here, we will discuss how the characteristics of LDDs, observed using the dependency decay curves result in perplexity values of different recurrent neural architectures. Table 2 lists the perplexity scores for test and valid sets for PTB, WikiText2 and WikiText103. There is a general trend in that model evaluations on WikiText103 tend to result in lower perplexity scores followed by WikiText2 and then PTB across a model. We are interested in understanding how the characteristics of the dataset (in particular properties of the LDDs in the data) affect the performance of recurrent neural architectures. With this goal in mind we analysed the attributes of the word-based natural language datasets. In order to examine the characteristics of the LDDs within each of these datasets we plotted the dependency decay curves indicating the decay of mutual information within the dataset as the spacing between the words is increased.

Dependency decay curves of the word-based natural language datasets follow expected trends [22]. It is seen that dependencies decay with a broken power-law [8] as explained in section 3.3.1. For word-based datasets, we observe that $\alpha 1 > \alpha 2$. The higher value of $\alpha 1$ is due to a higher rate of reduction in the frequency of contextually correlated words in a sequence, as the spacing between them increases. This signifies the presence of a strong grammar. This strong dependence is observed between words at a distance up to 4 across various datasets. For a given dataset, beyond the point of inflection, it is understood that the pairs are not contextually correlated which results in a flatter curve or lower value of $\alpha 2$. This analysis enables us to approximate the *contextual boundary* of the natural language data. Also, the absolute of value of mutual information is an indicator of the degree of the short and long distance dependencies present in a dataset. The fact that our above analysis of the English datasets found a very large value for $\alpha 1$ indicates that a dataset with good distribution of English text will exhibit a high value of mutual information at lower values of d followed by a steep decay of mutual information. As discussed above, we noted a trend in the results reported across the standard benchmark datasets where WikiText103 tended to deliver the best perplexity score followed by WikiText2 and PTB. Our analysis of the dependency decay curves provide an explanation for this trend. Language models have

Model	PTB	WikiText2	WikiText103
FRAGE + AWD-LSTM-MoS + dynamic eval [42]	$47.38, 46.54$	$40.85, 39.14$	-
AWD-LSTM-DOC x5 [43]	$48.63, 47.17$	$54.19, 53.09$	-
AWD-LSTM-MoS + dynamic eval [44]*	$48.33, 47.69$	$42.41, 40.68$	-
AWD-LSTM + dynamic eval [45]*	$51.6, 51.1$	$46.4, 44.3$	-
AWD-LSTM + continuous cache pointer [46]*	$53.9, 52.8$	-	-
AWD-LSTM-DOC [43]	$54.12, 52.38$	$53.8, 52.0$	-
AWD-LSTM-MoS + finetune [44]	$56.54, 54.44$	-	-
AWD-LSTM-MoS [44]	$58.08, 55.97$	$63.88, 61.45$	-
AWD-LSTM [46], 2017)	$60.0, 57.3$	$68.6, 65.8$	-
Transformer with tied adaptive embeddings [47]	-	-	$19.8, 20.5$
LSTM + Hebbian + Cache + MbPA [48]	-	-	$29.0, 29.2$

Table 2: Perplexity scores (test and valid) of SOTA word-based language models

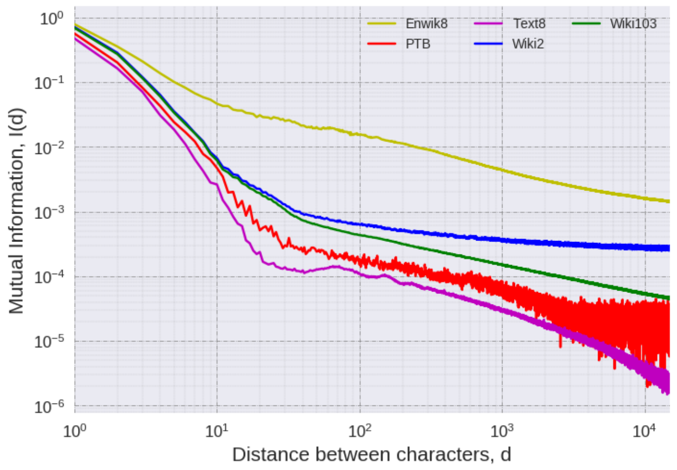

Figure 3: Dependency decay: Character-based dataset

very good performance on WikiText103 due to the fact that they can take advantage of large $\alpha 1$ and very low mutual information in the flat region. Furthermore, language models marginally outperform on WikiText2 as compared to the PTB due to the higher mutual information at lower values of d.

3.4 Dependency Decay Curves of Character-Based Datasets

In this section, we will study the dependency decay curve of character-based PTB, WikiText2, WikiText103, Text8, and Enwik8 datasets. They are displayed in Fig. 3. Dependency decay curves of character-based natural language datasets follow expected trends [49]. As observed in word-based datasets, even the character-based datasets exhibit broken power-law dependence decay, an exception being Enwik8 (which we will discuss later). For character-based datasets, strong dependence (steeper dependence decay) is observed between characters at a distance up to 30; beyond which it follows a long tail indicating lower dependence. Enwik8 displays a different decay characteristics than the other datasets as this dataset is made up of XML format and not English text. When we fit the dependency decay curve, we observe that it is made up of 4 constituent power-laws.

3.5 Dependency Decay Curves of Mobility Dataset

We also computed the dependency decay curves of the GPS trajectory dataset collected in Geolife project (Microsoft Research Asia) by 178 users in a period of over four years (from April 2007 to October 2011) and was plotted in Fig. 4. A GPS trajectory of this dataset is represented by a sequence of time-stamped points, each of which contains the information of latitude, longitude and altitude which was converted to a unique location number. These trajectories were recorded by different GPS loggers and GPS phone [50]. Upon analyzing the plot of the dependency decay curves in this data, it's evident that human mobility also has power law-decay suggesting the presence of LDDs.

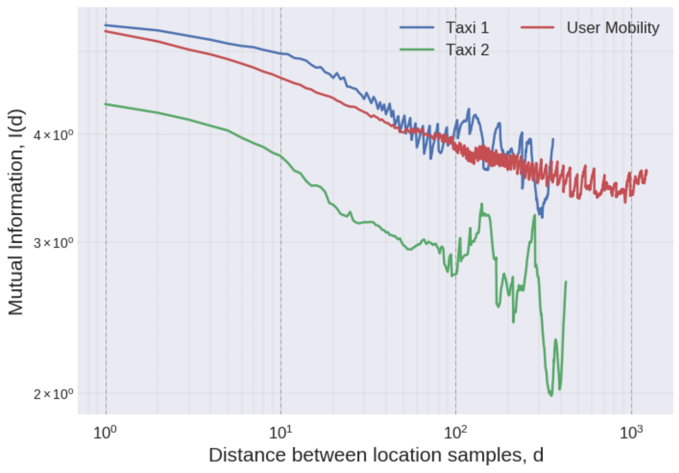

Figure 4: Dependency decay: Human mobility dataset

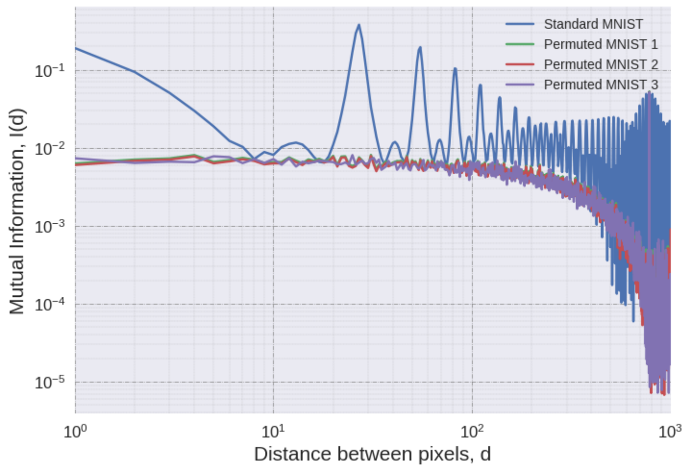

Figure 5: Dependency decay: Unpermuted *sequential MNIST* & permuted *sequential MNIST* using multiple seeds

3.6 Dependency Decay Curves of Sequential MNIST Dataset

Sequential MNIST is widely used to evaluate recurrent neural architectures. It contains 240000 training and 40000 test images. Each of these is 28x28 pixels in size, and each pixel can take one of 256 pixel values. In order to use them in a sequential task, the 2D images are converted into a 1D vector of 784 pixels by concatenating all the rows of the pixels. This transformation results in pixel dependencies which span up to approximately 28 pixels. These dependencies arise due to high correlation of a pixel with its neighboring pixels. The structure of the Sequential MNIST dataset is such that its dependency decay curve is likely to contain regular peaks and troughs. We plot the dependency decay curve of the unpermuted and permuted sequential MNIST datasets in Fig. 5.

Standard sequential MNIST exhibits high MI at $d=1$ indicating strong dependencies at close proximity. The dependencies then decay as a function of power-law. Hence, in-order to fully capture these dependencies, the recurrent neural architectures should maintain gradients/attention across multiple timescales as a function of power-law to accurately model these dependencies. However, we see peaks of mutual information at intervals of 28 due to pixel dependencies. The regular peaks in the decay curve indicate that the span of the dependencies lie within $d \approx 28$. We generated permuted versions of the sequential MNIST dataset with multiple seeds for use as a comparator with the unpermuted sequential MNIST. When we examine the dependency decay curves of permuted MNIST datasets, we observe that the dependencies are substantially less between close-by symbols (pixels in this case), e.g. for $d=1$ the green, red and purple lines are much lower than the blue line. This is a result of permutations applied to the data which disrupt spatial dependencies. Another impact of this disruption is the relatively flat curve for $d<300$ which indicates an absence of spatial dependencies. In-order to model these datasets that exhibit a relatively flat curve, the recurrent neural

Table 3: Results for sequential MNIST using GRU cells

# of Layers	Set of Dilations	Hidden per Layer	Accuracy
4	$1, 2, 4, 8$	$20/50$	$98.96/99.18$
5	$1, 2, 4, 8, 16$	$20/50$	$98.94/99.21$
6	$1, 2, 4, 8, 16, 32$	$20/50$	$\mathbf{99.17/99.27}$
7	$1, 2, 4, 8, 16, 32, 64$	$20/50$	$99.05/99.25$
8	$1, 2, 4, 8, 16, 32, 64, 128$	$20/50$	$99.15/99.23$
9	$1, 2, 4, 8, 16, 32, 64, 128, 256$	$20/50$	$98.96/99.17$

Table 4: Results for permuted sequential MNIST using RNN cells

# of Layers	Set of Dilations	Hidden per Layer	Accuracy
7	$1, 2, 4, 8, 16, 32, 64$	$20/50$	$95.04/95.94$
8	$1, 2, 4, 8, 16, 32, 64, 128$	$20/50$	$95.45/95.88$
9	$1, 2, 4, 8, 16, 32, 64, 128, 256$	$20/50$	$95.5/96.16$
10	$1, 2, 4, 8, 16, 32, 64, 128, 256, 512$	$20/50$	$95.62/96.4$
11	$1, 2, 4, 8, 16, 32, 64, 128, 256, 512, 780$	$20/50$	$\mathbf{95.66/96.47}$

architectures requires uniform distribution of attention/gradients across all time scales. However, beyond $d>300$, we observe exponential decay of dependence, where the value of MI falls below 10^{-5} indicating no further dependencies. This point ($d\approx 780$) indicates the span of the dependencies.

3.6.1 Experiments with Dilated Recurrent Neural Networks

Recurrent neural architectures always deliver better performance on unpermuted sequential MNIST as compared to permuted sequential MNIST. Our analysis of the dependency decay curves of these datasets provides an explanation for why this is the case. Unpermuted sequential MNIST has LDDs of less than 30, due to the period nature of pixel dependencies as explained in section 3.6. Datasets possessing such short-range dependency can be easily modeled using simple models as they don't require long memory. In the case of permuted sequential MNIST, we observe LDDs of more than 780 (due to exponential decay beyond that). Here, we use DilatedRNNs to train unpermuted and permuted sequential MNIST datasets in a classification task (classify digits 0-9 from their images). DilatedRNNs use multi-resolution dilated recurrent skip connections to extend the range of temporal dependencies in every layer and upon stacking multiple such layers are able to learn temporal dependencies at different scales [10]. This stacking of multi-resolution layers helps in passing contextual information over long distances which otherwise would have vanished via a single layer. Thus, the set of the dilations should, ideally, be tailored to match the dependency decay curves present in the dataset, and, in particular, the max dilation should match the max LDDs present in the dataset. The dilations per layer, and the number of layers, within a DilatedRNN are controlled by hyper-parameters [10].

The original paper that introduced DilatedRNNs [10] used the same max dilation hyper-parameter for both of these datasets i.e. 256, and a standard set of dilations (i.e., $1, 2, 4, 8, \dots$). The best results reported by [10] for these two datasets were: unpermuted sequential MNIST 99.0/99.2 and permuted sequential MNIST 95.5/96.1. However, our analysis of these datasets has revealed different max dependencies across these dataset. For unpermuted sequential MNIST we identified a periodicity of 28 and so we expected the max dilation value to be near 28 to deliver better performance. In permuted sequential MNIST we identified that the dependencies extend up to 780 and so we would expect better performance by extending the max dilation up to this value. To test these hypotheses we trained DilatedRNNs with various sets of dilations. To keep our results comparable with those reported in [10] the original code[1] was kept unchanged except for the max dilation hyper-parameter. The test results of these experiments are in tables 3 and 4. For unpermuted task, the model delivered best performance for max dilation of 32. Focusing on the results of the permuted sequential MNIST, the best performance was delivered with the max dilation of 780. These results confirm that the best performance is obtained when the max dilation is similar to the span of the LDDs of a given dataset.

[1] `https://github.com/code-terminator/DilatedRNN`

4 Computing Dependency Decay Curves of Artificial Datasets

Natural datasets present little to no control over the factors the affect LDDs. This, limits our ability to understand LDDs in more detail. Strictly k-Piecewise Languages (SPk) languages exhibit some types of LDDs occurring in natural datasets. Moreover, by modifying the SPk grammar we can control the dependency decay curves within a dataset generated by the grammar. To understand and validate the interaction between an SPk grammar and the LDD properties of the data we use a number of SPk grammars to generate datasets and analyse the properties of these datasets. Below is the description of the SPk language.

4.1 Strictly k-Piecewise Languages (SPk)

SPk languages form a subclass of regular languages. Subregular languages can be identified by mechanisms much less complicated than Finite-State Automata. Many aspects of human language such as local and non-local dependencies are similar to subregular languages [34]. More importantly, there are certain types of long distance (non-local) dependencies in human language which allow finite-state characterization [35]. These type of LDDs can easily be characterized by SPk languages and can be easily extended to other processes.

A language L, is described by a finite set of unique symbols Σ and Σ^* (*free monoid*) is a set of finite sequences or strings of zero or more elements from Σ.

Example 4.1. Consider, Σ = {σ_1, σ_2, σ_3, σ_4} where σ_1, σ_2, σ_3, σ_4 are the unique symbols. A *free monoid* over Σ contains all concatenations of these unique symbols. Thus, Σ^* = {λ, σ_1, $\sigma_1\sigma_2$, $\sigma_1\sigma_3$, $\sigma_1\sigma_4$, $\sigma_3\sigma_2$, $\sigma_3\sigma_1\sigma_3$, $\sigma_2\sigma_1\sigma_4\sigma_3$, ... }.

Definition 4.1. Let, u denote a string, e.g. u= $\sigma_3\sigma_2$. The length of a string u is denoted by $|u|$, and if u= $\sigma_3\sigma_2$ then $|u|$=2. A string with length zero is denoted by λ.

Definition 4.2. A string v is a *subsequence* of string w, iff $v = \sigma_1\sigma_2 \ldots \sigma_n$ and $w \in \Sigma^*\sigma_1\Sigma^*\sigma_2\Sigma^* \ldots \Sigma^*\sigma_n\Sigma^*$, where $\sigma \in \Sigma$. A *subsequence* of length k is called a *k-subsequence*. Let subseq$_k(w)$ denote the set of subsequences of w up to length k.

Example 4.2. Consider, Σ = {a, b, c, d}, w = [$acbd$], u = [bd], v = [acd] and x = [db]. String u is a *subsequence* of length k = 2 or *2-subsequence* of w. String v is a *3-subsequence* of w. However, string x is *not a subsequence* of w as it does not contain [db] subsequence.

SPk languages are defined by grammar G_{SPk} as a set of permissible *k-subsequences*. Here, k indicates the number of elements in a dependency. Datasets generated to simulate 2 elements in a dependency will be generated using SP2. This is the simplest dependency structure. There are more complex chained-dependency structures which require higher k grammars.

Example 4.3. Consider L, where Σ = {a, b, c, d}. Let G_{SP2} be SPk grammar which is comprised of permissible *2-subsequences*. Thus, G_{SP2} = {aa, ac, ad, ba, bb, bc, bd, ca, cb, cc, cd, da, db, dc, dd}. G_{SP2} grammar is employed to generate SP2 datasets.

Definition 4.3. Subsequences which are not in the grammar G are called *forbidden subsequences*[2].

Example 4.4. Consider Example 4.3, although {ab} is a possible *2-subsequence*, it is not part of the grammar G_{SP2}. Hence, {ab} is a *forbidden subsequence*.

Example 4.5. Consider strings u, v, w: u = [$bbcbdd$], v = [$bbdbbbcbddaa$] and w = [$bbabbbcbdd$], where $|u|$ = 6, $|v|$ = 12 and $|w|$ = 10. Strings u and v are valid SP2 strings because they are composed of subsequences that are in G_{SP2}. However, w is an invalid SP2 string because w contains {ab} a subsequence which is a *forbidden subsequence*. These constraints apply for any string x where $|x| \in \mathbb{Z}$.

Example 4.6. Let G_{SP3} = {aaa, aab, abb, baa, bab, bba, bbb, ...} and *forbidden subsequence* = {aba} be an SP*3* grammar which is comprised of permissible 3-*subsequences*. Thus, u = [$aaaaaaab$], where $|u|$ = 8 is a valid SP*3* string and v = [$aaaaabaab$], where $|v|$ = 9 is an invalid SP*3* string as defined by the grammar G_{SP3}.

The maximum extent of LDD exhibited by a certain SPk language is equal to the length of the strings generated which abide by the grammar. However, as per definition 4.2, the strings generated using this method will also exhibit dependencies of shorter lengths. It should be noted that the length of the LDD is not the same as k. The length of the LDD is the maximum distance between two elements in a dependency, whereas k specifies the number of elements in the dependency (as defined in the the SPk grammar).

[2]Refer section *5.2. Finding the shortest forbidden subsequences* in [20] for method to compute *forbidden sequences* for SPk language

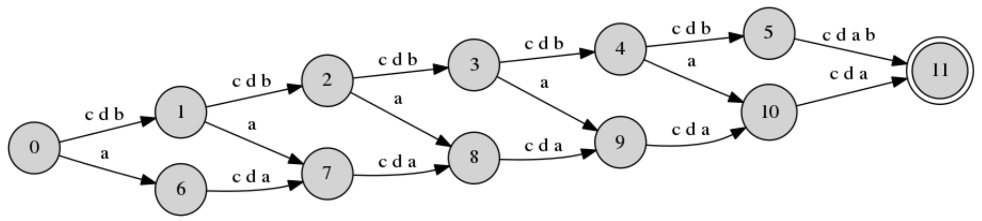

Figure 6: The automaton for G_{SP2} where n_l=6

Example 4.7. As per Example 4.5, v = [*bbdbbbcbddaa*], consider b in the first position, *subsequence* $\{ba\}$ exhibits dependency of 10 and 11. Similarly, *subsequence* $\{bd\}$ exhibits dependency of 2, 9, 10, etc.

Fig. 6 depicts a finite-state diagram of G_{SP2}, which generates strings of synthetic data. Consider a string x from this data, $\forall$ generated strings x generated using grammar G_{SP2}: $|x|$ = 6. The *forbidden subsequence* for this grammar is $\{ab\}$. Since $\{ab\}$ is a *forbidden subsequence*, the state diagram has no path (from state 0 to state 11) because such a path would permit the generation of strings with $\{ab\}$ as a subsequence, *e.g.* $\{abcccc\}$ Traversing the state diagram generates valid strings *e.g.* $\{$*accdda, caaaaa*$\}$.

Various $G_{SP\text{k}}$ could be used to define an SPk depending on the set of *forbidden subsequences* chosen. Thus, we can construct rich datasets with different properties for any SPk language. *forbidden subsequences* allow for the elimination of certain logically possible sequences while simulating a real world dataset where the probability of occurrence of that particular sequence is highly unlikely. Every SPk grammar is defined with at least one *forbidden subsequence*.

4.2 Dependency decay curves of SP*k* datasets

In-order to analyse the impact of vocabulary size on dependency decay curves, we generated SP2 grammars where $\Sigma_1 = \{a, b, c, d\}$ (size of vocabulary = 4) and $\Sigma_2 = \{a, b, c, d, ..., x, y, z\}$ (size of vocabulary = 26). We generated strings of maximum length of $20, 100, 200$ and 500 using SP2 grammar. As explained in Example 4.6, by increasing the length of the generated strings, the distance between dependent elements is also increased, resulting in longer LDDs. We can then simulate LDD lengths as $20, 100, 200$ and 500. We also choose two sets of forbidden strings for SP2 grammar, $\{ab, bc\}$ and $\{ab, bc, cd, dc\}$. We also generate two sizes of the same SP2 grammar to study the impact of the size of the data on the dependency decay curves, where one dataset was twice the size of the other. The datasets were generated using *foma* [51] and *python* [36]. Fig. 7 shows plots of the dependency decay curves of these datasets.

4.2.1 Impact of Dependency Length

Fig. 7a plots dependency decay curves of SP2 languages with maximum string length of $20, 100, 200,$ and 500. The point where dependency decay is faster, the *inflection point*, lies around the same point on *x-axis* as the maximum length of the LDD. This confirms that SPk can generate datasets with varying lengths of LDDs.

4.2.2 Impact of *k* - Multi-Element Dependency

Fig. 7b plots the dependency decay curves of SP2, SP*4* and SP*16* grammars. The strings in all the grammars are up to 100. Hence, we can observe the mutual information decay beyond D>100. k defines the number of correlated or dependent elements in a dependency rule. As k increases the grammar becomes more complex and there is an overall reduction in frequency of the dependent elements in a given sequence (due to lower probability of these elements occurring in a given sequence). Hence, the mutual information is lower. This can be seen with dataset of SP*16* vs SP2 and SP*4*. It is worth noting that datasets with lower mutual information curves tend to present more difficulty during modeling [36].

4.2.3 Impact of Vocabulary Size

The impact of vocabulary size can be seen in Fig. 7c where the dependency decay curves of SP2 datasets with vocabulary size (V) 4 and 26 are plotted. Both these datasets contain strings of maximum length 20. Hence the mutual information decays at 20. Both curves have identical decay indicating a similar grammar. However the overall mutual information of the dataset with $V = 26$ is much lower then the mutual information of the dataset with $V = 4$. This is because a smaller vocabulary results in an increase in the probability of the occurrence of each elements of occurrence of elements.

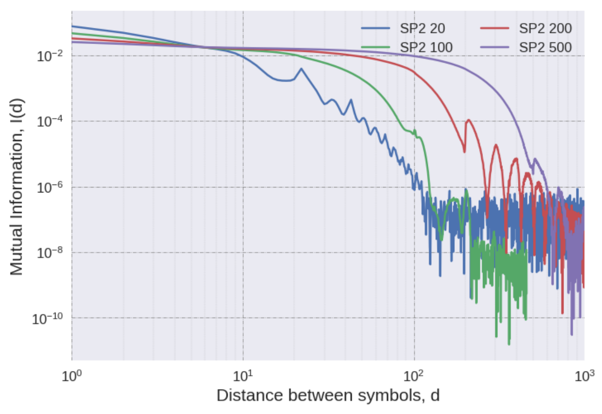

(a)

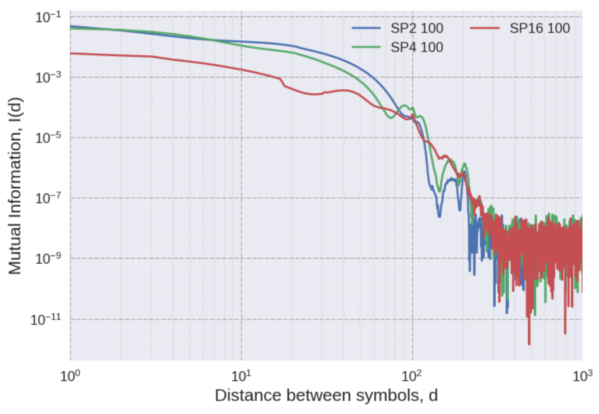

(b)

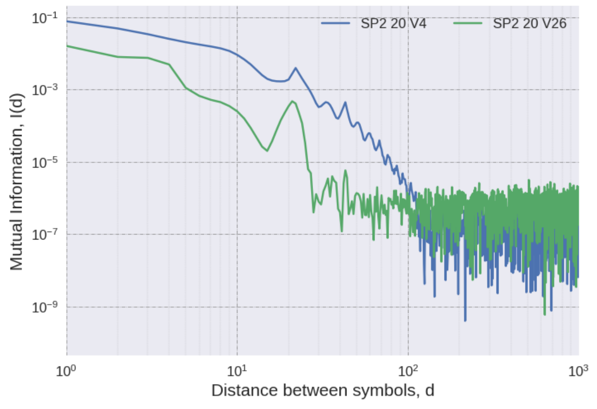

(c)

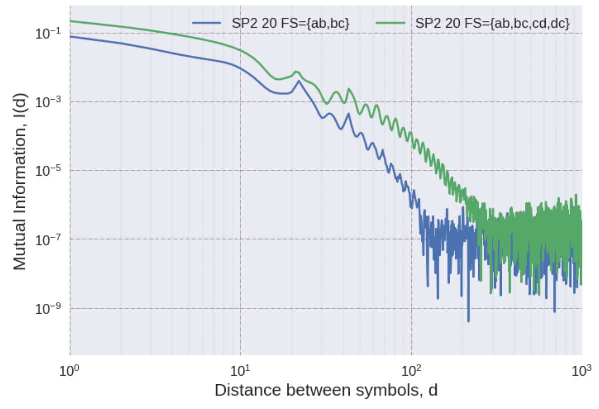

(d)

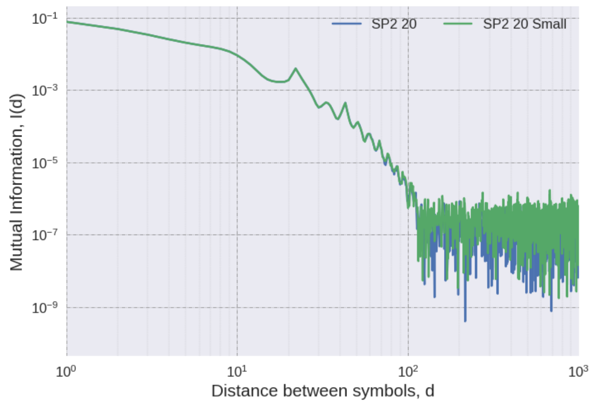

(e)

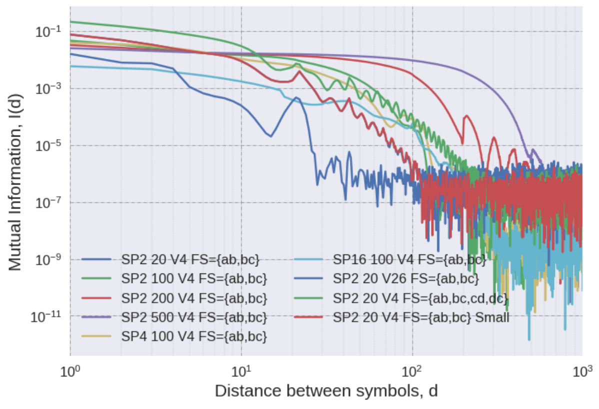

(f)

Figure 7: Dependency decay curves of datasets of (a) SP*2* grammar exhibiting LDDs of length 20, 100, 200, and 500. (b) SP*2*, SP*4* and SP*16* grammar exhibiting LDD of length 100. (c) SP*2* grammar with vocabulary of 4 and 26. (d) SP*2* grammar with varying forbidden strings (e) SP*2* grammar with varying size of the datasets (f) All the SP*k* grammars in a plot

4.2.4 Impact of Forbidden Strings

Fig. 7d plots the dependency decay curves of SP2 grammar with two set of *forbidden strings* as $\{ab, bc\}$ and $\{ab, bc, cd, dc\}$. It is seen that the dataset with more forbidden strings exhibited less steeper mutual information decay than the one with less number of forbidden strings. This can be attributed to the fact that datasets with more complex forbidden strings tend to exhibit more complex grammar as explained in section 4.1. By introducing more number of forbidden strings, it is possible to synthesize more complex LDDs as seen in the plot. In Fig. 7e we can observe the impact of the size of the dataset sampled from the same grammar. It can be seen that datasets sampled from the same grammar are less likely to be affected by the size of the dataset.

5 Discussion

The dependency decay curves of a dataset enable the visualisation of certain type of grammar in the dataset. For example, our analysis of word-based and character-based datasets in sections (3.3) and 3.4, indicate that the word-based grammar is very different from character-based grammar. Understanding the properties of the underlying grammar that produces a sequence can aid in choosing best recurrent neural architecture to learn that grammar. For example, the maximum length of LDDs is much smaller in word-based datasets as compared to character-based datasets. But at the same time word-based dependency decay curves exhibit higher value of overall mutual information. This is why the sequential model that performs best on the word-based language modeling task will not necessarily be the best choice for the character-based language modeling task.

One implication of these experiments is that having multiple benchmark datasets from a single domain does not necessarily improve the experimental testing of a models ability to learn LDDs in the dataset. LDDs are fixed within a domain and sampling more datasets from that domain simply results in testing the model on LDDs with similar characteristics. Consequently, the relatively limited set of domains and tasks covered by benchmark datasets indicates that current benchmarks do not provide enough LDD variety to extensively test the capacity of recurrent neural architectures.

It can also be noted that even though a specific grammar does induce similar dependency decay curves, there are subtle variations. These variations depend on a number of factors such as size of the vocabulary, size of the dataset, dependency structure (for e.g. "*k*" and "*forbidden strings*") and presence of any other noisy data (or presence of another grammar as seen with *Enwik8* dataset). Thus, if a recurrent neural architecture intends to model a dataset, knowing these factors would greatly benefit in selecting the best hyper-parameters of the sequential model. Also, these artificial grammars allow for the generation of rich datasets by setting the parameter *k*, the maximum length of the strings generated, size of vocabulary and by choosing appropriate *forbidden substrings*. This presents a compelling case to use these grammars to benchmark state-of-the-art sequential models.

As seen in dependency decay curves of sequential MNIST, it is evident that the use of sequential MNIST in benchmark tasks is out of place due to the absence of long distance dependencies. This presents a compelling case to analyze dependency decay curves of benchmark datasets before they are selected for this job. Also, the presence of a flat curve with very low mutual information in permuted sequential MNIST dataset is usually a result of noisy data. It is this noisy data (rather than complex LDDs) that is responsible for reducing the performance of the recurrent neural architectures. Overall, however we would argue that both of these datasets are inadequate at benchmark sequential models due to their limitation in generating complex LDDs.

6 Conclusion

The major contribution of this paper represent a synthesis of distinct themes of research on LDDs from multiple fields, including information theory, artificial neural networks for sequential data modeling, and formal language theory. The potential impact of this synthesis for neural networks research include: an appreciation of the multifaceted nature of LDDs; a procedure for measuring dependency decay curves within a dataset; an evaluation and critique of current benchmark datasets and tasks for LDDs; an analysis of how the use of these standard benchmarks and tasks can be misleading in terms of evaluating the capacity of a neural architectures to generalize to datasets with different forms of LDDs; and, a deeper understanding of the relationship between hyper-parameters and LDDs within language model architectures which can directly contribute to the development of more accurate and efficient sequential models.

Acknowledgment

This research was partly supported by the ADAPT Research Centre, funded under the SFI Research Centres Programme (Grant 13/RC/2106) and is co-funded under the European Regional Development Funds. We gratefully acknowledge the support of NVIDIA Corporation with the donation of the Titan Xp GPU under NVIDIA GPU Grant used for this research.

References

[1] Jeffrey L. Elman. Finding structure in time. *COGNITIVE SCIENCE*, 14(2):179–211, 1990.

[2] Sepp Hochreiter. Untersuchungen zu dynamischen neuronalen netzen. Master's thesis, TU Munich, 1991.

[3] Sepp Hochreiter, Yoshua Bengio, and Paolo Frasconi. Gradient flow in recurrent nets: the difficulty of learning long-term dependencies. In J. Kolen and S. Kremer, editors, *Field Guide to Dynamical Recurrent Networks*. IEEE Press, 2001.

[4] Y. Bengio, P. Simard, and P. Frasconi. Learning long-term dependencies with gradient descent is difficult. *IEEE Transactions on Neural Networks*, 5(2):157–166, March 1994.

[5] Thomas M. Cover and Joy A. Thomas. *Elements of Information Theory*. Wiley-Interscience, New York, NY, USA, 1991.

[6] Liam Paninski. Estimation of entropy and mutual information. *Neural Computation*, 15(6):1191–1253, 2003.

[7] Gerlof Bouma. Normalized (pointwise) mutual information in collocation extraction. In *Proceedings of the Biennial GSCL Conference 2009*, 01 2009.

[8] Henry W. Lin and Max Tegmark. Critical behavior in physics and probabilistic formal languages. *Entropy*, 19(7), 2017.

[9] Salah El Hihi and Yoshua Bengio. Hierarchical recurrent neural networks for long-term dependencies. In *Proceedings of the 8th International Conference on Neural Information Processing Systems*, NIPS'95, pages 493–499, Cambridge, MA, USA, 1995. MIT Press.

[10] Shiyu Chang, Yang Zhang, Wei Han, Mo Yu, Xiaoxiao Guo, Wei Tan, Xiaodong Cui, Michael Witbrock, Mark A Hasegawa-Johnson, and Thomas S Huang. Dilated recurrent neural networks. In I. Guyon, U. V. Luxburg, S. Bengio, H. Wallach, R. Fergus, S. Vishwanathan, and R. Garnett, editors, *Advances in Neural Information Processing Systems 30*, pages 77–87. Curran Associates, Inc., 2017.

[11] Víctor Campos, Brendan Jou, Xavier Giró-i Nieto, Jordi Torres, and Shih-Fu Chang. Skip rnn: Learning to skip state updates in recurrent neural networks. In *International Conference on Learning Representations*, 2018.

[12] Sepp Hochreiter and Jürgen Schmidhuber. Long short-term memory. *Neural computation*, 9(8):1735–1780, 1997.

[13] Stephen Merity, Caiming Xiong, James Bradbury, and Richard Socher. Pointer sentinel mixture models. *CoRR*, abs/1609.07843, 2016.

[14] A. Graves, G. Wayne, and I. Danihelka. Neural Turing Machines. *ArXiv e-prints*, October 2014.

[15] Giancarlo D. Salton, Robert J. Ross, and John D. Kelleher. Attentive language models. In *IJCNLP*, 2017.

[16] Ashish Vaswani, Noam Shazeer, Niki Parmar, Jakob Uszkoreit, Llion Jones, Aidan N Gomez, Ł ukasz Kaiser, and Illia Polosukhin. Attention is all you need. In I. Guyon, U. V. Luxburg, S. Bengio, H. Wallach, R. Fergus, S. Vishwanathan, and R. Garnett, editors, *Advances in Neural Information Processing Systems 30*, pages 5998–6008. Curran Associates, Inc., 2017.

[17] Zihang Dai, Zhilin Yang, Yiming Yang, William W. Cohen, Jaime Carbonell, Quoc V. Le, and Ruslan Salakhutdinov. Transformer-XL: Language modeling with longer-term dependency, 2019.

[18] Mitchell Marcus, Grace Kim, Mary Ann Marcinkiewicz, Robert MacIntyre, Ann Bies, Mark Ferguson, Karen Katz, and Britta Schasberger. The penn treebank: Annotating predicate argument structure. In *Proceedings of the Workshop on Human Language Technology*, HLT '94, pages 114–119, Stroudsburg, PA, USA, 1994. Association for Computational Linguistics.

[19] James Rogers, Jeffrey Heinz, Gil Bailey, Matt Edlefsen, Molly Visscher, David Wellcome, and Sean Wibel. On Languages Piecewise Testable in the Strict Sense. In Christian Ebert, Gerhard Jäger, and Jens Michaelis, editors, *The Mathematics of Language*, pages 255–265, Berlin, Heidelberg, 2010. Springer Berlin Heidelberg.

[20] Jie Fu, Jeffrey Heinz, and Herbert G. Tanner. An algebraic characterization of strictly piecewise languages. *Lecture Notes in Computer Science (including subseries Lecture Notes in Artificial Intelligence and Lecture Notes in Bioinformatics)*, 6648 LNCS:252–263, 2011.

[21] Enes Avcu, Chihiro Shibata, and Jeffrey Heinz. Subregular complexity and deep learning. In *Proceedings of the Conference on Logic and Machine Learning in Natural Language (LaML)*, 2017.

[22] W Ebeling and T Pöschel. Entropy and long-range correlations in literary english. *Europhysics Letters (EPL)*, 26(4):241–246, may 1994.

[23] C. K. Peng, S. V. Buldyrev, A. L. Goldberger, S. Havlin, F. Sciortino, M. Simons, and H. E. Stanley. Long-range correlations in nucleotide sequences. *Nature*, 356:168, Mar 1992.

[24] S. S. Melnik and O. V. Usatenko. Entropy and long-range correlations in dna sequences. *Computational biology and chemistry*, 53 Pt A:26–31, 2014.

[25] N. Chomsky. Three models for the description of language. *IRE Transactions on Information Theory*, 2(3):113–124, September 1956.

[26] Noam Chomsky. On certain formal properties of grammars. *Information and Control*, 2(2):137–167, 1959.

[27] W Tecumseh Fitch and Angela D Friederici. Artificial grammar learning meets formal language theory: an overview. *Philosophical Transactions of the Royal Society B: Biological Sciences*, 367(1598):1933–1955, jul 2012.

[28] Arthur S. Reber. Implicit learning of artificial grammars. *Journal of Verbal Learning and Verbal Behavior*, 6(6):855–863, 1967.

[29] M. Casey. The dynamics of discrete-time computation, with application to recurrent neural networks and finite state machine extraction. *Neural Computation*, 8(6):1135–1178, Aug 1996.

[30] A. W. Smith and D. Zipser. Encoding sequential structure: experience with the real-time recurrent learning algorithm. In *International 1989 Joint Conference on Neural Networks*, pages 645–648 vol.1, 1989.

[31] Masaru Tomita. Learning of construction of finite automata from examples using hill-climbing : RR : Regular set Recognizer. *Proceedings of Fourth International Cognitive Science Conference*, pages 105–108, 1982.

[32] Raymond L. Watrous and Gary M. Kuhn. Induction of finite-state automata using second-order recurrent networks. In *NIPS*, 1991.

[33] C. L. Giles, C. B. Miller, D. Chen, H. H. Chen, G. Z. Sun, and Y. C. Lee. Learning and extracting finite state automata with second-order recurrent neural networks. *Neural Computation*, 4(3):393–405, May 1992.

[34] G. Jager and J. Rogers. Formal language theory: refining the Chomsky hierarchy. *Philosophical Transactions of the Royal Society B: Biological Sciences*, 367(1598):1956–1970, 2012.

[35] Jeffrey Heinz and James Rogers. Estimating strictly piecewise distributions. In *Proceedings of the 48th Annual Meeting of the Association for Computational Linguistics*, ACL '10, pages 886–896, Stroudsburg, PA, USA, 2010. Association for Computational Linguistics.

[36] Abhijit Mahalunkar and John D. Kelleher. Using regular languages to explore the representational capacity of recurrent neural architectures. In Věra Kůrková, Yannis Manolopoulos, Barbara Hammer, Lazaros Iliadis, and Ilias Maglogiannis, editors, *Artificial Neural Networks and Machine Learning – ICANN 2018*, pages 189–198, Cham, 2018. Springer International Publishing.

[37] Claude Elwood Shannon and Warren Weaver. *The mathematical theory of communication*. University of Illinois Press, Urbana, 1949.

[38] Robert M. Fano. *Transmission of Information: A Statistical Theory of Communication*. MIT Press, Cambridge, MA, USA, 1961.

[39] P. Grassberger. Entropy Estimates from Insufficient Samplings. *ArXiv Physics e-prints*, July 2003.

[40] James E. Rhoads. The dynamics and light curves of beamed gamma-ray burst afterglows. *The Astrophysical Journal*, 525(2):737–749, nov 1999.

[41] Gudlaugur Jóhannesson, Gunnlaugur Bjöörnsson, and Einar H. Gudmundsson. Afterglow light curves and broken power laws: A statistical study. *The Astrophysical Journal Letters*, 640(1):L5, 2006.

[42] Chengyue Gong, Di He, Xu Tan, Tao Qin, Liwei Wang, and Tie-Yan Liu. Frage: Frequency-agnostic word representation. In *Proceedings of the 32nd International Conference on Neural Information Processing Systems*, NIPS'18, page 1341–1352, Red Hook, NY, USA, 2018. Curran Associates Inc.

[43] Sho Takase, Jun Suzuki, and Masaaki Nagata. Direct output connection for a high-rank language model. In *Proceedings of the 2018 Conference on Empirical Methods in Natural Language Processing*, pages 4599–4609. Association for Computational Linguistics, 2018.

[44] Zhilin Yang, Zihang Dai, Ruslan Salakhutdinov, and William W. Cohen. Breaking the softmax bottleneck: A high-rank RNN language model. In *International Conference on Learning Representations*, 2018.

[45] Ben Krause, Emmanuel Kahembwe, Iain Murray, and Steve Renals. Dynamic evaluation of neural sequence models. In Jennifer Dy and Andreas Krause, editors, *Proceedings of the 35th International Conference on Machine Learning*, volume 80 of *Proceedings of Machine Learning Research*, pages 2766–2775, Stockholmsmässan, Stockholm Sweden, 10–15 Jul 2018. PMLR.

[46] Stephen Merity, Nitish Shirish Keskar, and Richard Socher. Regularizing and optimizing LSTM language models. In *International Conference on Learning Representations*, 2018.

[47] Alexei Baevski and Michael Auli. Adaptive input representations for neural language modeling. In *International Conference on Learning Representations*, 2019.

[48] Jack Rae, Chris Dyer, Peter Dayan, and Timothy Lillicrap. Fast parametric learning with activation memorization. In Jennifer Dy and Andreas Krause, editors, *Proceedings of the 35th International Conference on Machine Learning*, volume 80 of *Proceedings of Machine Learning Research*, pages 4228–4237, Stockholmsmässan, Stockholm Sweden, 10–15 Jul 2018. PMLR.

[49] Marcelo A. Montemurro and Pedro A. Pury. Long-range fractal correlations in literary corpora. *Fractals*, 10(04):451–461, 2002.

[50] Yu Zheng, Hao Fu, Xing Xie, Wei-Ying Ma, and Quannan Li. *Geolife GPS trajectory dataset - User Guide*, July 2011.

[51] Mans Hulden. Foma: a finite-state compiler and library. In *Proceedings of the 12th Conference of the European Chapter of the Association for Computational Linguistics*, pages 29–32. Association for Computational Linguistics, 2009.